Original Article

Naringenin Sensitizes Resistant C6 Glioma Cells with a Repressive Impact on the Migrating Ability

Annals of Neurosciences
27(3-4) 114–123, 2020

DOI: 10.1177/0972753120950057
journals.sagepub.com/home/aon
SAGE

Jayalakshmi J[1] and Arambakkam Janardhanam Vanisree[1]

Abstract

Background: Glioma, the most common form of a malignant brain tumour is characterised by a poor prognosis, which is attributable to its resistance against current therapeutic approaches. Temozolomide (TMZ), a DNA alkylating agent, is the first-line drug for glioma treatment. Long-term treatment using TMZ was reported to culminate in the development of resistance with overexpression of multidrug resistance 1 gene coded protein P-glycoprotein, which in turn releases the drugs from the tumour cells.

Purpose: Thus, to circumvent such resistance issues, the current study attempted to explore the effect of naringenin (a flavanone) with proven antiglial tumour potential, in mitigating the features of TMZ resistance.

Methods: Colony-forming assay, invasion assay and scratch wound assay were performed among the groups, namely tumour control (C6), vehicle control (V), naringenin (NGEN)-treated, drug-resistant tumour cells (C6R), and drug resistance cells added with NGEN (C6R+NGEN), to examine the impact of NGEN on migration and invasion. The effect of NGEN on filopodia length and density during cell migration was also studied in addition to the matrix metalloproteinases (MMP-2 and MMP-9) and p-ERK levels.

Results and Conclusion: NGEN and C6R+NGEN groups had shown significant reduction ($P < .01$) in length and density of filopodia, colony formation, invasion and wound healing. Further, NGEN could also modify the assessed protein levels ($P < .001$), which were involved in migration and invasion in sensitive and resistant cells. Our study had provided the first evidence on NGEN-induced enhanced sensitivity against TMZ resistance with profound influence as an antimigratory and anti-invasive agent.

Keywords

Drug resistance, P-glycoprotein, naringenin, F-actin, filopodia

Introduction

Inherent or acquired resistance to cytotoxic agents remains a supreme obstacle for the effective treatment of human cancers. Gliomas, the common intracranial brain tumours, are one among devastating cancers with median survival rate of 12 to15 months owing to multidrug resistance. This necessitates a research focus on modes that can overcome the issue of resistance. The key characters of multidrug resistance are the development of cross resistance to drugs, which are functionally and structurally unrelated,[1] and/or impaired accumulation of drug in resistance cells compared to their sensitive counterpart.[2] In addition to this, overexpression of P-glycoprotein (P-gp), a membrane glycoprotein coded by the gene multidrug resistance 1 (*MDR1*), is observed with multidrug resistance.[3] Drug retention is decreased mainly because of enhanced active drug efflux from resistant cells, which is manifested via P-gp.[4]

In tumour progression, particularly in metastasis, invasion and drug resistance play the most important roles.[5] Invasion and development of drug resistance are related processes, as they share signalling pathways.[6,7] The major cause for the failure of treatment strategies in glioma is because of uncontrolled migration and invasion of glioma cells from the tumour region. Extracellular signal-regulated Kinase (ERK) is one of the key molecules of Mitogen Activated Protein Kinase (MAPK) pathway, responsible for invasion of the cancer cells by primarily breaking down the extracellular matrix (ECM). MAPKs regulate the proteolytic

[1] Department of Biochemistry, University of Madras, Chennai, Tamil Nadu, India

Corresponding author:
Arambakkam Janardhanam Vanisree, Department of Biochemistry, University of Madras, Chennai, Tamil Nadu 600005, India.
E-mail: journalsvuom@gmail.com

enzymes in the surroundings that degrade the basement membrane via p-ERK, resulting in the destruction of ECM, a key histological marker of invasive cancer.

Further, there are classes of endopeptidases that are notably involved in cancer cell migration and invasion. Secretion of such matrix metalloproteinases (MMPs), a zinc-dependent endopeptidases family, has been reported to be associated with the degree of malignancy of brain tumors as they degrade ECM components, thus paving the way for invasion.[8] In many cancer types such as melanoma, breast, prostate and brain cancers, elevated levels of MMP9 were found accompanied by increased metastatic potential.[9] In addition to MMPs, migration and invasion of tumour cells require dynamic reorganisation of the actin cytoskeleton.[10,11] Membrane protrusions produced by migrating cells, such as lamellipodia, filopodia, focal adhesions, invadopodia and stress fibres are important for migration and invasion. The formation of filopodia is considered to be an essential process in the migration of cells as it acts as a major sensing element of the extracellular microenvironment. Filopodia is an extension of cell membrane, which forms initial contact with the ECM, these structures are mainly regulated by polymerisation and depolymerisation of actin. The major process in the migration of cell is the reorganisation of actin microfilaments into strong bundles of actin micrrofilaments in parallel in filopodium.[12–15] It was shown that the regulation of actin polymerisation and filamentous actin (F-actin) formation in the migrating edge of glioblastoma cells may inhibit its migration and invasion.[10]

In this context, therapeutic strategies that can effectively control resistance, invasion and migration behaviour of glioma cells need to be explored. Naringenin (NGEN), a bioflavonoid, belongs to the flavanone subclass. It is found in citrus fruits, grapes and tomatoes. Earlier we have shown the anti-glial effect of NGEN,[16,17] purportedly by downregulating the PI3K/Akt kinases.[18] These findings have led to the current study design which aims to explore the effect of NGEN on levels of MMPs, invasion, migration, and also to uncover its impact on filopodia length and density in temozolomide (TMZ) sensitive and resistance glioma cells.

Materials and Methods

Reagents

NGEN was purchased from Sigma Aldrich. The antibodies used in this study were as follows: MMP2 (Santa Cruz Biotechnology, sc-13594), MMP 9 (Santa Cruz Biotechnology, sc-6840), pErk (Santa Cruz Biotechnology, sc-377400), MAPK (Erk1/2), antibody (Cell Signalling Technology #9102), and β-actin (Santa Cruz Biotechnology, sc47778).

C6 Glioma Cell Lines

Rat C6 glioma cell line was procured from the NCCS, Pune, India, and was maintained at 37° C with 5% CO_2 and 95% air. DMEM medium was used for culturing the cells added with fetal bovine serum (FBS; 10%) as a supplement; the antibiotics used were penicillin-G (50 unit/mL) and streptomycin (50 µg/mL).

Cell Viability Assay

The viability of cells was measured by MTT assay.[19] 5×10^2 cells were plated in a 96-well plate with DMEM supplemented with 10% FBS at 37° C under 5% CO_2, 95% O_2. After 12 h of incubation, the complete medium was changed with serum free medium. After 24 h, the control cells were added with 0.01% DMSO containing medium and treatment cells were added with 50–350 µM of NGEN containing DMEM medium, 100–700 µM of Doxorubicin (Dox) and 200–1200 µM of TMZ containing medium. After 24 h, 100 µL of 0.5% MTT was added and incubated for 4 h at 37° C. Then MTT was replaced by 100 µL of solubilising solution (acid isopropanol), the colour developed was read at 650 nm. The percentage of cell viability was calculated, plotted and the IC_{50} value for NGEN and TMZ was observed.

Development of TMZ Resistance Cell

TMZ resistance C6 cells (C6R) were established by treating C6 cells with 600 µmol/L (IC_{50} = 600 – 800 µmol/L) of TMZ for eight months. During this eight-month period, TMZ containing media was replaced at three day intervals.[20] The quantification of the resistance level (RL) of C6R cells was represented by the ratio of IC_{50} of resistance cells to the IC_{50} of their sensitive counterpart.

Rhodamine 123 (Rh123) Efflux Assay

3×10^6 cells were suspended in 2 mL of Rh123 (100 ng/mL) at 37° C for 60 min. Followed by the incubation, the cells were washed thrice with cold Hanks Balanced Salt Solution (HBSS) for five min each time. Then the cells were resuspended in HBSS dye (Rh123) free medium with or without standard P-gp blockers (5 µM verapamil) or NGEN (250 µM) at 37° C for 30 min. After incubation, the fluorescence intensity was measured flow cytometrically at 530/30 nm in CytoFLEX Beckman Coulter.[21]

Experimental Groups

Experimental groups incorporated in the study included

- Group I. C6 cells, which served as control.
- Group II. C6 glioma cells were treated with 0.1% DMSO and served as vehicle control.
- Group III. C6 treated with 250 µM of NGEN in 0.1% dimethyl sulfoxide (DMSO).
- Group IV. C6R-multidrug resistance C6 cells developed by growing in 600 µM TMZ containing medium for a period of five months.

- Group V. C6R treated with 300 μM of NGEN in 0.1% DMSO.

Scratch Wound Heal Assay

The scratches for creating wounds were done by scraping the confluent monolayer culture using a T200 pipette tip. Photographs were taken at 0 and 24 h and the images were analysed using Image J software. More than five wound healing areas for all the groups were photographed and the average wound heal was calculated. The percent of wound closure was found by taking wound area at 0 h as100%.

Matrigel Invasion Essay

The cells were treated with NGEN for 24 h after that they were seeded on the matrigel coated top chambers (Millipore). Serum containing DMEM medium was added in the lower chamber after 48 h of incubation, the top chamber containing non-invaded cells were removed with a cotton swab and the cells invaded to the lower surface were fixed with 4% paraformaldehyde for 15 min. The cells were then washed with PBS thrice and stained with 0.2% crystal violet for 10 min and the cells were photographed.

Anchorage-Independent Growth in Soft Agar

One percent agarose in DMEM was pipetted into a 6-well plate and allowed to solidify. 0.6% agarose in DMEM and cell suspension (1×10^4) in a 1:1 ratio were added over the bottom layer of agarose and allowed to solidify. A layer of DMEM containing 10% FBS with or without NGEN (250μm/mL) was maintained over the upper layer of agarose to prevent desiccation. The medium was changed twice in a week for a period of 21 days, after which, the colonies were detected by staining with 0.005% crystal violet; the images were photographed.[22] The experiment was repeated thrice and the average number of colonies in each group was determined using Image J software.

Western Blot Analysis

Cells were homogenised with homogenising buffer and the total protein levels were quantified using Bradford method. The homogenate containing 50μg of total protein was boiled in Laemmli buffer for five min then loaded and separated by electrophoresis at room temperature in polyacrylamide gel. After separation, the gels were electroblotted on PVDF membrane at 150mA and blocked using 5% BSA at room temperature for 3 h. The membrane was washed with TBS-T and incubated with the diluted primary antibodies in TBS-T at 4° C for 12 h: MAPK (Erk 1/2) (1:1000), p-ERK (1:1000), MMP2 (1:1000), MMP 9 (1:1000) and β-actin (1:1000). The membranes were washed thrice with TBS-T and incubated with diluted horseradish peroxidase conjugated secondary antibodies (1:2000) at room temperature for 1 h and the proteins were detected using DAB reagent. The band intensity was calculated using an image J software.

Isolation of RNA for qRT PCR

For the total RNA extraction, 5×10^4 cells were used using TRIZOL reagent (Takara, Japan). mRNA levels of MAPK, p-ERK , MMP2, MMP 9 and β-actin were detected with real-time PCR system (Bio-Rad Laboratories) using SYBR Green master mix (Takara, Japan). The sequence for, MMP2 is Forward 5' AGAAGGCTGTGTTCTTCGCA 3', Reverse 5' AAAGGCAGCGTCTACTTGCT 3', for MMP9 is Forward 5' GATCCCCAGAGCGTTACTCG 3' Reverse 5' GTTGTGGAAACTCACACGCC 3', for MAPK1 is Forward 5' CATTGTCTCACTGTGTTGCCA 3' Reverse 5' CCAGGAAAGTCAGAAGGCACT 3' and for β-actin is Forward 5' CTCTGTGTGGATTGGTGGCT 3' and backward 5' CGCAGCTCAGTAACAGTCCG 3'. The cycle threshold (Ct) values were determined using qbase PLUS software. Ct value of target gene and reference gene (β-actin) were used to calculate their corresponding ΔCT. The ΔΔCT value of relative quantification was carried out to find the fold changes in expression (ΔΔCT = ΔCT target – ΔCT reference).

Filamentous Actin (F-Actin) Staining

C6 cells were plated on 15 mm glass coverslip coated with Poly L Lysine. The scratches were done by scraping across the cells using a T200 pipette and washing the well thrice with PBS. Low-serum DMEM containing either NGEN or 0.1% DMSO was added. After 8 h, the medium was discarded and added with 70% ice-cold ethanol to fix the cell for 10 min. Then the cells were permeabilise with 0.1% Triton X-100 for 5 min. The F-actin was stained with Phalloidin-iFluor 488 Reagent—cytopainter of Abcam for 20–60 min and washed with PBS thrice. Then the coverslips were mounted using fluoroshield and the confocal fluorescence image was obtained with ZEISS LSM 700 microscope. Filopodia number, density and length were analysed using AnalyzeSkeleton algorithms and Skeletonize3D of Fiji Image J software (FiloQuant). Filopodia density was quantified by the ratio of filopodia number to edge length (obtained using software).

Statistical Analysis

All the data were processed with GraphPad Prism software. The results were expressed as mean ± SEM. One-way ANOVA followed by Tukeys's post hoc test and Dunnett's multiple comparison test were carried out to compare the multiple samples. $P < .05$ was considered statistically significant.

Results

Effects of NGEN and TMZ on Viability of C6 Glioma Cells

C6R cells were established by treating C6 cells with TMZ for a period of eight months. The effect of Dox, NGEN and TMZ on cell viability of C6 and C6R cells were studied by MTT assay at various concentrations (100–700 µM) for Dox, (50–350 µM) for NGEN, and (200–1200 1) for TMZ for 24 h. Dox was used to confirm the multidrug resistance nature of TMZ mediated resistant C6R cells. A comparison of cell viability between C6 and C6R after a 24-h treatment had shown significant differences in their sensitivity to Dox, NGEN and TMZ (Figure 1). A considerable decrease in C6 cell viability was obtained with 400 µM Dox, 250 µM NGEN and 700 µM TMZ, while a significant effect of Dox, NGEN and TMZ in C6R cells was evident at 600 µM, 300 µM and 900 µM, respectively. C6R cell line exhibited a 42.8% increase in the RL when compared to its sensitive counterpart C6 cell line (Table 1).

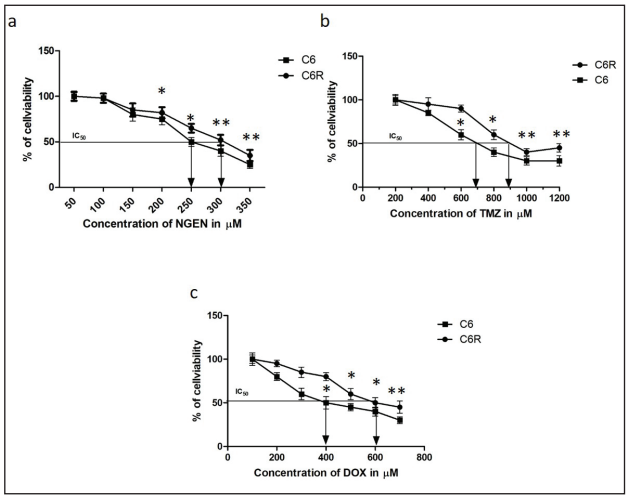

Figure 1. Cell viability assay. (a and b) Effect of Naingenin and Temozolomide on cell viability of C6 and C6R cells treated with increasing concentrations of Naringenin (50–350 µM) and Temozolomide (200–12000 µM) for 24 h. (c) Sensitivity to Doxorubicin among C6 and C6R cells with increasing concentrations of Doxorubicin (100–700 µM) (n = 3).

Note: * $P < .05$, ** $P < .03$.

Table 1. Results of the Viability Index (IC_{50}) and the Resistance Level (RL) of the Parent C6 Cell Line (C6) and the Chemoresistant Cells (C6R)

Cell Line	IC_{50}	Resistant Level (RL)
C6	700 µM	1.00
C6R	1000 µM	1.428

Flow Cytometric Functional Release of Rh123

Figure 1 is the flow cytometric representation of release of Rh123 histograms in C6 sensitive (C6) (blue histogram) and drug-resistant (C6R) (red histogram). Rh123 efflux from the cell totally depends on P-gp expression and reflects the multidrug resistance of cells; thus, Rh123 was used to study the P-gp mediated resistance. C6 cell lines are shown in Figure 2 along with their respective standard P-gp blocker (verapamil)-treated cells (C6+V, C6R+V) and NGEN-treated cells (C6+NGEN, C6R+NGEN). The intensity histogram shift from right to left demonstrated the rapid release of the drug Rh123 by C6R cell line and it was reversed by NGEN. After an incubation of 30 min in a dye-free medium, there was a rapid reduction of Rh123 fluorescence in resistant cells when compared with the incubation in NGEN containing medium.

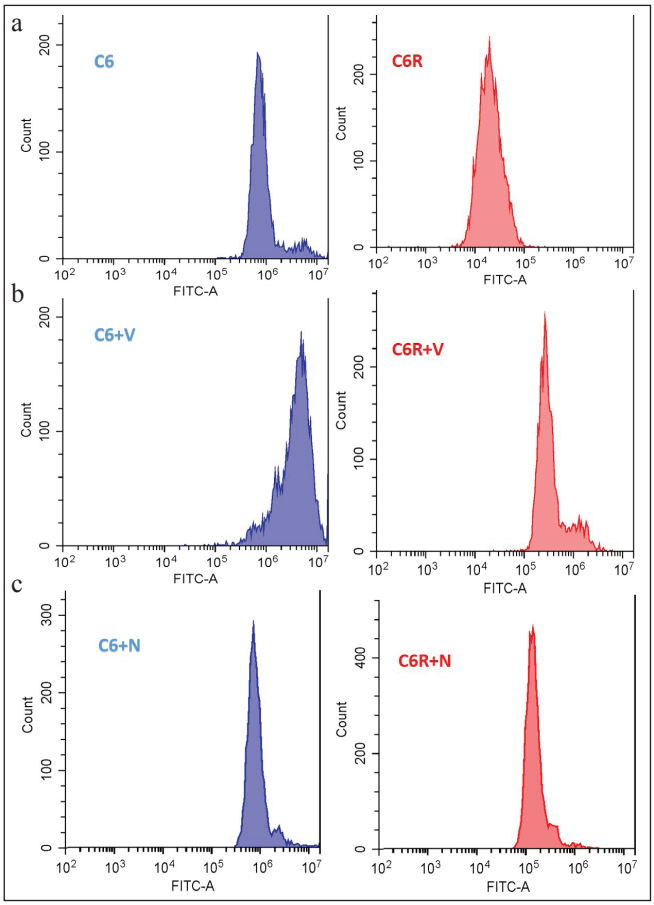

Figure 2. Flowcytometric histograms representing efflux of Rh123 in C6 sensitive (blue histograms) and C6 resistant (C6R) (red histograms) cell line. (a) 30 min incubation with Rh123 in dye-free medium, (b) 30 min incubation with Rh123 in dye-free medium containing verapamil (C6+V and C6R+V), (c) on 30 min incubation with Naringenin (C6+N and C6R+N).

Effect of NGEN on Cell Migration

Scratch wound heal assay was carried out to evaluate the effect of NGEN on cell migration (Figure 3). The distances between the boundaries of the wound region were measured and compared at 0 h and at 24 h using Image J software. The distance at 0 h was considered as 100%. The results confirmed that the migration capacity of untreated C6 and resistant cells was significantly higher at 24 h when compared with NGEN-treated cells ($P < .01$).

Effect of NGEN on Anchoring Independent Colony Formation

Soft agar assay was carried out to assess the impact of NGEN on colony formation by the cells (Figure 4). After 21 days of maintenance of culture, C6 cells and resistant cells displayed a greater number of colonies when compared to NGEN-treated cells ($P < .001$). This suggested that NGEN could reverse the colonogenicity of C6 and resistant tumour cells in anchorage-independent soft agar medium.

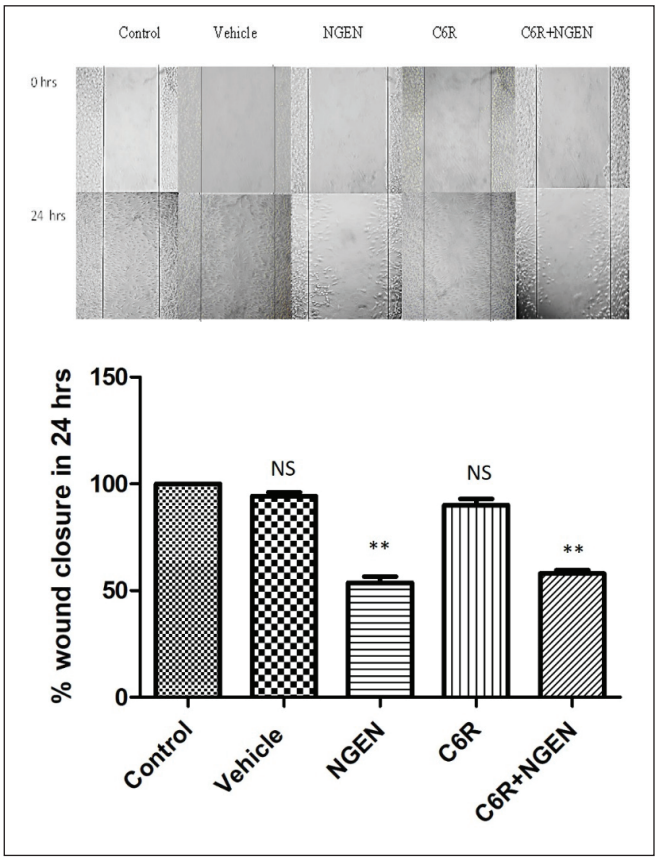

Figure 3. Representation of wound closure assay. Cell migration was captured at 0 h and 24 h (original magnification, ×20). Mean migration distance of the experimental groups to its relative control group were represented by bar graphs.

Abbreviations: NS, nonsignificant.

Note: ** $P < .01$, $n = 3$.

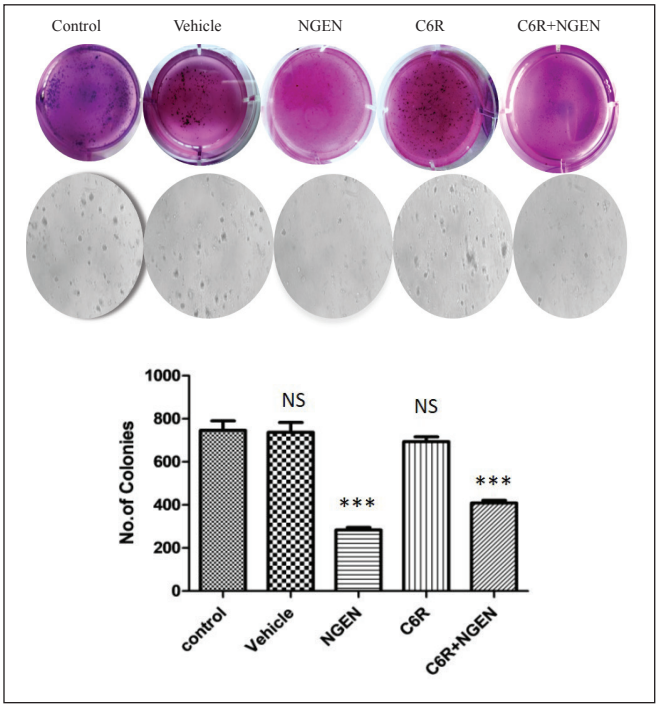

Figure 4. The effect of Naringenin on colony formation in soft agar. After 21 days of colony formation in soft agar, colonies were stained with 0.005% crystal violet and the images were photographed. No. of colonies were determined using Image J software. The results were expressed as (mean ± SD).

Abbreviations: NS, nonsignificant.

Note: ***$P < .001$ vs control group (untreated cells); $n = 3$.

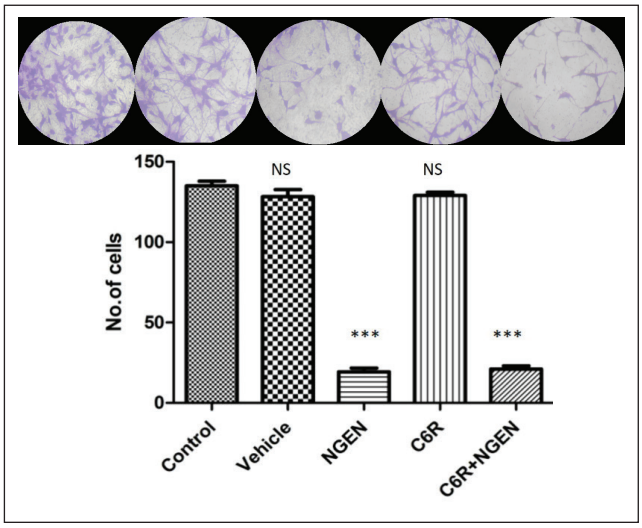

Figure 5. Representative images of Matrigel transwell invasion assays. Invaded cells were stained with crystal violet and the images were photographed. Bar graphs represent the mean number of invaded cells from random fields (mean ± SD).

Abbreviations: NS, nonsignificant, $n = 3$.

Note: ***$P < .001$ vs control group (untreated cells).

Effect of NGEN on tumour Invasion

Transwell inserts precoated with Matrigel were used to assess the invasion. The number of cells that invaded through the Matrigel in NGEN-treated C6 and C6R cells were significantly lower ($P < .001$) than the cells that were untreated (Figure 5).

NGEN Inhibits mRNA Levels and Expression of p-ERK, MMP-2 and -9

MMP-2 and MMP-9, ECM proteins, have been reported to enhance the tumour cell migration, invasion and growth via p-ERK activation. To investigate whether NGEN could suppress p-ERK, MMP-2 and MMP-9, we have performed qRT-PCR to find mRNA levels, and western blot analysis to investigate their corresponding levels of protein. Densitometric data from western blot by image J showed that the treatment of C6 glioma cells and C6R-resistant cells with NGEN could significantly reduce ($P < .05$) the expression of proteins like p-ERK, MMP-2 and MMP-9 (Figures 6A and B). Also, mRNA levels were significantly reduced ($P < .001$) among NGEN-treated groups of sensitive and resistant C6 cells (Figure 6C).

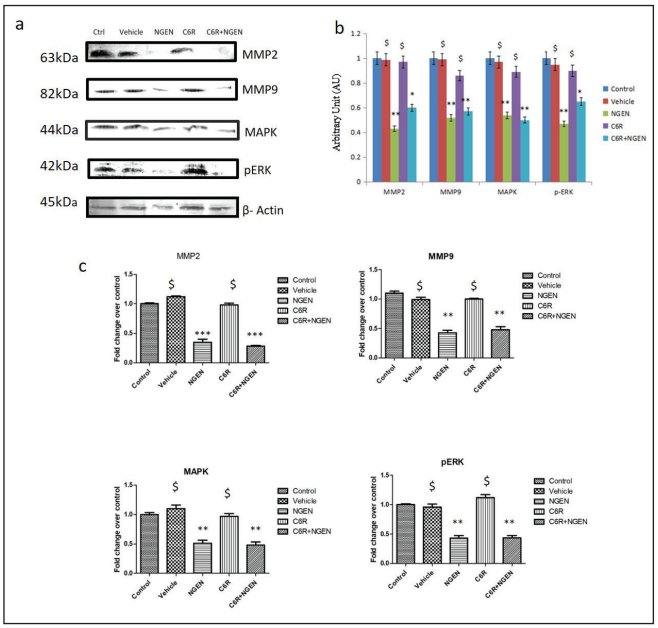

Figure 6. (a) Immunoblot data of MMP2, MMP 9, MAPK, p-ERK and β-actin in control and experimental groups. (b) Densitometric data of the bands normalised with β-actin. (c) Data on qRT PCR analysis between control and experimental groups. ANOVA was performed using the mean fold change (over β-actin) compared to that of control.

Abbreviations: NS, nonsignificant.

Note: *** ($P < .001$), ** ($P < .01$), *($P < .05$); $n = 3$.

Filopodia in Migration

F-actin engaged in the regulation of membrane protrusion at the leading edge of motile cells. In the current study, the effect of NGEN on filopodia number, length, and density in C6 and C6R cells was investigated. In Figure 7A, C6 and C6R cells showed elongated thin morphology of filopodia at the migrating edge, whereas, NGEN-treated C6 and C6R cells showed rounded morphology, thus NGEN establishing its impact on filopodia formation and cell migration. From the data it was found that the number, length and density of filopodia were significantly ($P < .001$, $P < .01$ and $P < .05$, respectively; Figures 7B and 7C) reduced in NGEN-treated sensitive and resistant cells.

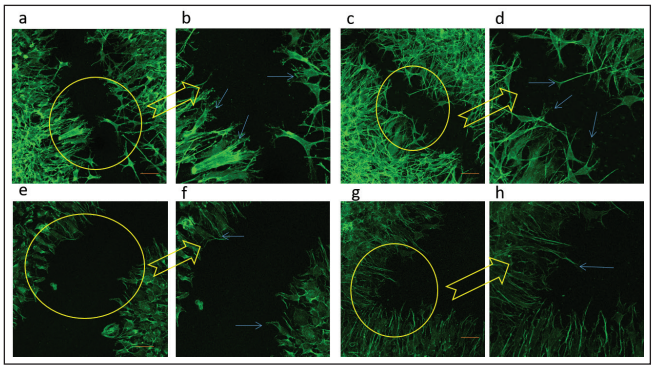

Figure 7A. Confocal imaging of the leading edge of migrating cells stained with F-actin by Phalloidin. Encircled parts of figure a, c, e and g are magnified and shown in figure b, d, f and h (20×). a and b are Control, c and d are C6R, e and f are NGEN-treated, g and h are C6R+NGEN . Blue arrows represent the filopodia formation at the leading edge of migrating cells. Scale bar, 20 μm (a, c, d, g) 5 μm (b, d, f, h).

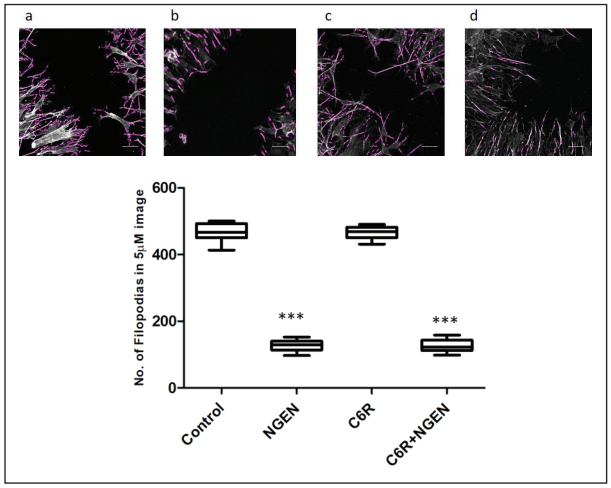

Figure 7B. Quantification of filopodia numbers using the FiloQuant plug-in of FIJI Image J software were highlighted in magenta colour and were displayed as Tukey box plots. One way ANOVA was carried out and followed by Dunnett's multiple comparison test. *** $P < .001$. Scale bar, 5 μm. (a) control, (b) NGEN, (c) C6R, (d) C6R+NGEN.

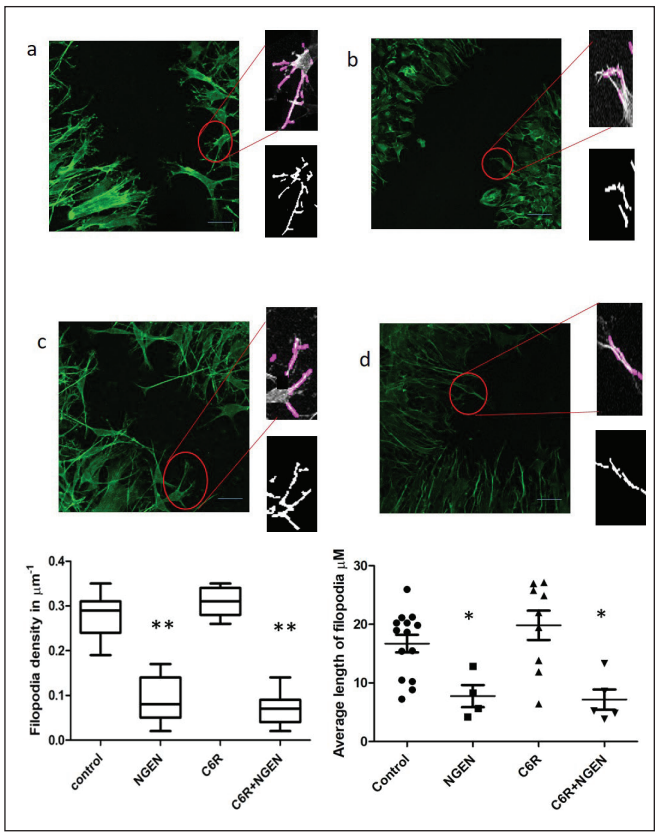

Figure 7C. Filopodia density and average length at the migrating edge. Filopodia density and length were analysed using Fiji Image J software. In the inset image one of the cell with filopodium at the migrating edge was highlighted in magenta in the top image and its corresponding skeleton image at the bottom were obtained from software. Filopodia density was quantified by the ratio of filopodia number to edge length (obtained using software). Filopodia density and mean length were compared between the migrating cell of all the groups. Results were displayed as Tukey box plots and dot plot. One way ANOVA followed by Dunnett's multiple comparison test were carried out. ** $P < .01$ * $P < .05$, $n = 3$. Scale bar, 5 µm (a) control, (b) NGEN, (c) C6R, and (d) C6R+NGEN.

Discussion

NGEN, a bioflavonoid found in citrus fruit, is said to possess numerous biological and pharmacological properties which mainly include anticancer properties.[16–18] The detailed molecular mechanism of the anti-invasive activity of NGEN is yet to be identified. To the best of our knowledge, there are no reports yet about the anti-invasive and the anti-metastatic ability of NGEN against resistant C6 (C6R) cells. In this study, we have characterised the impact of NGEN against the migration and invasion of C6 cells and multidrug-resistant C6R cells. Long-term treatment with TMZ results in drug resistance by profound reprogramming of the genomic and transcriptomic changes in proliferation, migration and invasion. We have established drug resistance glioma cell line C6R from its sensitive counterpart, C6 glioma cell line. The resistance was induced by TMZ, a commonly used drug for treatment of glioma in humans. The drug resistance of C6R phenotype to a DNA alkylating agent Dox, other than TMZ, was also confirmed by cell viability assay. In the results, we have depicted an increase in IC_{50} for TMZ and Dox when compared to the sensitive C6 counterpart.

The drug resistance of C6R was also confirmed using the Rh123 efflux assay. The functional release of Rh123 is totally dependent on the MDR1 expression and it reflects the multidrug resistance of the cells. After 30 min of incubation in a dye-free (Rh123) medium, the C6R cells exhibited a decrease in the fluorescence intensity of Rh123, and measured flow cytometrically, when compared to that of C6 cells (Figure 2A). This made evident an increased efflux of Rh123 by C6R cells compared to C6 cells. The drug/dye efflux is the phenomenon of the cell with elevated expression of P-gp in the resistant cells which pumps out the fluorescent drug that aid in identifying drug resistance.[21] We performed a reversal of Rh123 efflux by blocking the P-gp using Verapamil, a standard PGP inhibitor and found that both the control and resistant cells showed an increase in the fluorescent intensity of Rh123 when incubated with verapamil containing medium for 30 min and exhibiting its effect as blockers (Figure 2B). Similarly, both the C6 and C6R cells were incubated with NGEN for 30 min[23] and this also exhibited the retention of Rh123 in the cell with a subsequent increase in the fluorescent intensity of Rh123 and thus demonstrating its effect as blockers (Figure 2C).

We have encountered the drastic effect of NGEN on migration and invasion potential of C6 and C6R cells. From the scratch wound closure study (Figure 3), we have demonstrated attenuated migration of C6 and C6R cells treated with NGEN (250 µM) when compared to that of C6 and C6R. Supporting our observation, the anti-migratory potential of NGEN in various cancer cell lines was reported.[24,25] The citrus flavonoids were shown to suppress the migration and invasion capacity of cancer cells via downregulation of MMPs.[25–27] The recent findings of Chen et al.[28] had also shown the anti-migratory and anti-invasion properties of NGEN through various mechanisms including MMPs, ERK, p38 and EMT markers on glioma cells. In line with such reports, this study also had revealed that NGEN-treated cells shown a significant reduction in invasion and MMP levels. The levels of MMP-2 and MMP-9 were assessed in this study using Western blot analysis (expression) (Figure 6) and had shown attenuated levels of MMP-2 and MMP-9 in C6 and C6R glioma cells upon NGEN treatment. ECM degradation helps in invasion and metastasis of cancer. Especially, MMP2 and MMP9 play a crucial role in the degradation of ECM.[29] MMP2 and MMP9 were reported to be active in glioma patients compared to those of normal and were said to be correlated with poor prognosis.[30,31] The extensive range of cellular functions like proliferation, migration, survival and apoptosis are regulated by MAPKs.[32] Several studies have demonstrated that flavonoids reduce the migration of glioma cells by inhibiting MAPKs signals. For example, Quercetin,

Nobiletin and NGEN were found to diminish the migration and invasion of GBM cells via inhibition of MAPKs including ERK.[33,34,28] In line with such reports, the current study had shown that NGEN could inhibit the expression of MAPK and pERK and suppress the migration of C6 and C6R cells. Based on such observations, we demonstrated that NGEN can significantly inhibit the migration and invasion of C6 and C6R cells, partly by downregulating MAPK, pERK, MMP-2 and MMP-9. The data leads to an assumption that NGEN may build an efficient therapeutic strategy against invasion and migration of malignant gliomas.

Encouraged by our observation on migration and invasion, we explored the effect of NGEN on filopodia formation, the cell protrusion which is essential for cell migration[12–15] of the C6 and C6R cells. From our results, it was evident that at the leading edge of filopodia, protrusion was prominent with elongated and thin in C6 and C6R cells (Figure 7). This filopodia formation enables the cells to migrate. Similar outcomes were obtained in the studies by Koh et al.,[35] where two types of filopodia migration at the leading edge of migrating cells, saltatory and continuous migration, were shown. A decade ago, in another report, it was demonstrated that decreased filopodia formation is accompanied by decreased migration,[36] establishing that filopodia plays a crucial role in the migration of control and resistance cells as noted in Figures 7A and C. Interestingly, we found that NGEN-treated C6 and C6R cells (Figure 7) show rounded morphology instead of elongated, thin morphology like C6 and C6R cells. Incomplete or lack of filopodia formation with unclear leading-edge protrusions were observed that can lead to poor migration. Very recently, Koh et al.35 had reported that the elongated cells with filopodia showed the migrating ability in heterogeneous morphology of patient-derived GBM cells, but rounded cells showed an irregular morphology, thus forming poorly-defined small protrusions and not well-defined filopodia at the migrating edge of the cell. Apart from the morphology of cells, we also found that there was a significant reduction in the filopodia numbers, length and density. According to Arjonen et al.,[37] filopodia stimulated the migration of cells in various cell types and enhanced filopodia density were shown in many cancer cells. In stick to such report, we found well-developed and better density of filopodium in C6 and C6R cells; whereas, NGEN-treated cells showed a significant reduction in density of filopodium and this might play a major part in cancer cell migration. According to many reports, filopodia has been directly involved in the invasion and metastasis of cancer cells.[38] The role of CCR3, sVEGFR1, MCP-1, stem cells, and herbs can also be explored.[40-47] Shibue et al.,[39] had shown that filopodium plays a crucial role in the mammary carcinoma cell invasion as it enters the lung parenchyma and interstitium-like environments. In light of such reports and our observation, we claim that NGEN can exert its impact on migration and invasion via filopodia formation.

To summarise, the current findings prove NGEN, an anti-tumour agent against C6 cells as it was found to repress the migration and invasion of C6 cells and drug resistance C6R cells through downregulation of protein kinases such as pErk/Mapk, MMP2 and MMP9. These findings are potentially important to develop therapeutic interventions against glioma. The anti-migratory potential of NGEN is further confirmed by a decreased formation of filopodia at the leading edge of migration. Though, these findings are considered potentially important to develop therapeutic interventions against glioma, the study on detailed molecular mechanisms, by which NGEN acts on actin and other cytoskeletal proteins that alter the formation of filopodia and glioma cell motility, will be subservient in furthering our knowledge on the role of NGEN in F-actin dynamics of migrating C6 glial cells.

Declaration of Conflicting Interests

The authors declared no potential conflicts of interest with respect to the research, authorship and/or publication of this article.

Ethical Statement

This study did not include any clinical samples or animal samples.

Funding

The authors disclosed receipt of the following financial support for the research, authorship, and/or publication of this article: This work was supported by the University Grants Commission under the award of UGC-BSR Meritorious fellowship (Grant no.: GCCO/a-2/UGCMERITORIOUS/2015/284), New Delhi, India.

References

1. Skovsgaard T. Mechanisms of resistance to daunorubicin in Ehrlich ascites tumor cells. Cancer Res June 1, 1978; 38(6): 1785–1791.
2. Danø K. Active outward transport of daunomycin in resistant Ehrlich ascites tumor cells. Biochim Biophys Acta-Biomembr October 25, 1973; 323(3): 466–483.
3. Gottesman MM, Fojo T, and Bates SE. Multidrug resistance in cancer: role of ATP–dependent transporters. Nature Rev Cancer January 2002; 2(1): 48–58.
4. Housman G, Byler S, Heerboth S, et al. Drug resistance in cancer: an overview. Cancers September 2014; 6(3): 1769–1792.
5. Krakhmal NV, Zavyalova MV, Denisov EV, et al. Cancer invasion: Patterns and mechanisms. Acta Naturae (англоязычная версия) 2015; 7(2): 17–28.
6. Alexander S and Friedl P. Cancer invasion and resistance: Interconnected processes of disease progression and therapy failure. Trends Mol Med January 1, 2012; 18(1): 13–26.
7. Häger A, Alexander S, and Friedl P. Cancer invasion and resistance. EJC Suppl September 2013; 11(2): 291.

8. Lin CW, Shen SC, Chien CC, et al. 12-O-tetradecanoylphorbol-13-acetate-induced invasion/migration of glioblastoma cells through activating PKCα/ERK/NF-κB-dependent MMP-9 expression. J Cell Physiol November 2010; 225(2): 472–481.
9. Moulik, S, Pal S, Biswas J, and Chatterjee A. Role of ERK in modulating MMP 2 and MMP 9 with respect to tumour invasiveness in human cancer cell line MCF-7 and MDA-MB-231. J Tumor 2014; 2(2): 87–98.
10. Nürnberg A, Kitzing T, and Grosse R. Nucleating actin for invasion. Nature Rev Cancer March 2011; 11(3): 177–187.
11. Hayashi K, Michiue H, Yamada H, et al. Fluvoxamine, an antidepressant, inhibits human glioblastoma invasion by disrupting actin polymerization. Sci Rep March 18, 2016; 6(1): 1–2.
12. Bartles JR. Parallel actin bundles and their multiple actin-bundling proteins. Curr Opin cell biol February 1, 2000; 12(1): 72–78.
13. Cohan CS, Welnhofer EA, Zhao L, Matsumura F, and Yamashiro S. Role of the actin bundling protein fascin in growth cone morphogenesis: Localization in filopodia and lamellipodia. Cell Motil Cytoskeleton February 2001; 48(2): 109–120.
14. Kureishy N, Sapountzi V, Prag S, Anilkumar N, and Adams JC. Fascins, and their roles in cell structure and function. Bioessays April 2002; 24(4): 350–361.
15. Adams JC. Roles of fascin in cell adhesion and motility. Curr Opinion cell Biol October 1, 2004; 16(5): 590–596.
16. Sabarinathan D, Mahalakshmi P, and Vanisree AJ. Naringenin promote apoptosis in cerebrally implanted C6 glioma cells. Mol Cell Biochem December 1, 2010; 345(1–2): 215–222.
17. Sabarinathan D, Mahalakshmi P, and Vanisree AJ. Naringenin, a flavanone inhibits the proliferation of cerebrally implanted C6 glioma cells in rats. Chem Biol Interact January 15, 2011; 189(1–2): 26–36.
18. Sabarinathan D and Vanisree AJ. Plausible role of naringenin against cerebrally implanted C6 glioma cells in rats. Mol Cell Biochem March 1, 2013; 375(1–2): 171–178.
19. Safadi FF, Xu J, Smock SL, et al. Expression of connective tissue growth factor in bone: Its role in osteoblast proliferation and differentiation in vitro and bone formation in vivo. J Cellular Physiol July 2003; 196(1): 51–62.
20. Munoz JL, Rodriguez-Cruz V, Greco SJ, Nagula V, Scotto KW, and Rameshwar P. Temozolomide induces the production of epidermal growth factor to regulate MDR1 expression in glioblastoma cells. Mol Cancer Ther October 1, 2014; 13(10): 2399–2411.
21. Petriz J and Garcia-Lopez J. Flow cytometric analysis of P-glycoprotein function using rhodamine 123. Leukemia July 1997; 11(7): 1124–1130.
22. Borowicz S, Van Scoyk M, Avasarala S, et al. The soft agar colony formation assay. JVisualized Exp October 2014; 27(92): e51998.
23. Bansal T, Jaggi M, Khar R, and Talegaonkar S. Emerging significance of flavonoids as P-glycoprotein inhibitors in cancer chemotherapy. J Pharm Pharm Sci April 6, 2009; 12(1): 46–78.
24. Chang HL, Chang YM, Lai SC, et al. Naringenin inhibits migration of lung cancer cells via the inhibition of matrix metalloproteinases-2 and-9. Exp Therc Med February 1, 2017; 13(2): 739–744.
25. Liao AC, Kuo CC, Huang YC, et al. Naringenin inhibits migration of bladder cancer cells through downregulation of AKT and MMP2. Mol Med Rep September 1, 2014; 10(3): 1531–1536.
26. Kawabata K, Murakami A, and Ohigashi H. Nobiletin, a citrus flavonoid, down-regulates matrix metalloproteinase-7 (matrilysin) expression in HT-29 human colorectal cancer cells. Biosci Biotechnol Biochem January 1, 2005; 69(2): 307–314.
27. Stagos D, Amoutzias GD, Matakos A, et al. Chemoprevention of liver cancer by plant polyphenols. Food Chem Toxicol June 1, 2012; 50(6): 2155–2170.
28. Chen YY, Chang YM, Wang KY, et al. Naringenin inhibited migration and invasion of glioblastoma cells through multiple mechanisms. Environ Toxicol March 2019; 34(3): 233–239.
29. Itoh Y and Nagase H. Matrix metalloproteinases in cancer. Essays Biochem 2002; 38: 21–36.
30. Musumeci G, Magro G, Cardile V, et al. Characterization of matrix metalloproteinase-2 and -9, ADAM-10 and N-cadherin expression in human glioblastoma multiforme. Cell Tissue Res 2015; 362: 45–60.
31. Ramachandran RK, Sorensen MD, Aaberg-Jessen C, Hermansen SK, and Kristensen BW. Expression and prognostic impact of matrix metalloproteinase-2 (MMP-2) in astrocytomas. PLoS One 2017; 12: e0172234.
32. Yang SH, Sharrocks AD, and Whitmarsh AJ. MAP kinase signalling cascades and transcriptional regulation. Gene 2013; 513: 1–13.
33. Lien LM, Wang MJ, Chen RJ, et al. Nobiletin, a Polymethoxylated flavone, inhibits glioma cell growth and migration via arresting cell cycle and suppressing MAPK and Akt pathways. Phytother Res 2016; 30: 214–221.
34. Pan HC, Jiang Q, Yu Y, Mei JP, Cui YK, and Zhao WJ. Quercetin promotes cell apoptosis and inhibits the expression of MMP-9 and fibronectin via the AKT and ERK signalling pathways in human glioma cells. Neurochem Int 2015; 80: 60–71.
35. Koh I, Cha J, Park J, Choi J, Kang SG, and Kim P. The mode and dynamics of glioblastoma cell invasion into a decellularized tissue-derived extracellular matrix-based three-dimensional tumor model. Sci Rep March 15, 2018; 8(1): 1–2.
36. Hwang JH, Smith CA, Salhia B, and Rutka JT. The role of fascin in the migration and invasiveness of malignant glioma cells. Neoplasia (New York, NY) February 2008; 10(2): 149.
37. Arjonen A, Kaukonen R, and Ivaska J. Filopodia and adhesion in cancer cell motility. Cell Adhes Migration September 1, 2011; 5(5): 421–30.
38. Caswell PT and Zech T. Actin-based cell protrusion in a 3D matrix. Trends Cell Biol October 1, 2018; 28(10): 823–834.
39. Shibue T, Brooks MW, Inan MF, Reinhardt F, and Weinberg RA. The outgrowth of micrometastases is enabled by the

formation of filopodium-like protrusions. Cancer Discovery August 1, 2012; 2(8): 706–721.

40. Sharma NK, Gupta A, Prabhakar S, Singh R, Bhatt AK, Anand A. CC chemokine receptor-3 as new target for age-related macular degeneration. Gene. 2013 Jul 1;523(1):106-11.
41. Anand A, Gupta PK, Sharma NK, Prabhakar S. Soluble VEGFR1 (sVEGFR1) as a novel marker of amyotrophic lateral sclerosis (ALS) in the North Indian ALS patients. European Journal of Neurology. 2012 May;19(5):788-92.
42. Kamal Sharma N, Gupta A, Prabhakar S, Singh R, Sharma S, Anand A. Single nucleotide polymorphism and serum levels of VEGFR2 are associated with age related macular degeneration. Current neurovascular research. 2012 Nov 1;9(4):256-65.
43. Anand A, Saraf MK, Prabhakar S. Sustained inhibition of brotizolam induced anterograde amnesia by norharmane and retrograde amnesia by l-glutamic acid in mice. Behavioural brain research. 2007 Aug 22;182(1):12-20.
44. Anand A, Saraf MK, Prabhakar S. Antiamnesic effect of B. monniera on L-NNA induced amnesia involves calmodulin. Neurochemical research. 2010 Aug 1;35(8):1172-81.
45. Mathur D, Goyal K, Koul V, Anand A. The molecular links of re-emerging therapy: a review of evidence of Brahmi (Bacopa monniera). Frontiers in pharmacology. 2016 Mar 4;7:44.
46. Anand A, Sharma NK, Gupta A, Prabhakar S, Sharma SK, Singh R, Gupta PK. Single nucleotide polymorphisms in MCP-1 and its receptor are associated with the risk of age related macular degeneration. PloS one. 2012 Nov 21;7(11):e49905.
47. Mathur D, Goyal K, Koul V, Anand A. The molecular links of re-emerging therapy: a review of evidence of Brahmi (Bacopa monniera). Frontiers in pharmacology. 2016 Mar 4;7:44.